Smart Structures and Systems, *Vol. 18, No. 3 (2016) 585-599*
DOI: http://dx.doi.org/10.12989/sss.2016.18.3.585

Force monitoring of steel cables using vision-based sensing technology: methodology and experimental verification

X.W. Ye*, C.Z. Dong[a] and T. Liu[b]

Department of Civil Engineering, Zhejiang University, Hangzhou 310058, China

(Received August 7, 2015, Revised November 3, 2015, Accepted March 1, 2016)

Abstract. Steel cables serve as the key structural components in long-span bridges, and the force state of the steel cable is deemed to be one of the most important determinant factors representing the safety condition of bridge structures. The disadvantages of traditional cable force measurement methods have been envisaged and development of an effective alternative is still desired. In the last decade, the vision-based sensing technology has been rapidly developed and broadly applied in the field of structural health monitoring (SHM). With the aid of vision-based multi-point structural displacement measurement method, monitoring of the tensile force of the steel cable can be realized. In this paper, a novel cable force monitoring system integrated with a multi-point pattern matching algorithm is developed. The feasibility and accuracy of the developed vision-based force monitoring system has been validated by conducting the uniaxial tensile tests of steel bars, steel wire ropes, and parallel strand cables on a universal testing machine (UTM) as well as a series of moving loading experiments on a scale arch bridge model. The comparative study of the experimental outcomes indicates that the results obtained by the vision-based system are consistent with those measured by the traditional method for cable force measurement.

Keywords: structural health monitoring; cable-supported bridge; cable force; vision-based system; digital image processing; pattern matching algorithm

1. Introduction

Steel cables are widely employed in long-span bridges such as cable-stayed bridges, suspension bridges, and arch bridges. Since they act as the main load-bearing components and play a vital role in ensuring the safety of bridge structures, accurate measurement of the tensile force of the steel cable has practical necessity and social significance during in-construction and in-service stages (Kim and Park 2007). Force monitoring of the steel cable is becoming one of the most important issues in the field of structural health monitoring (SHM), which has been a cutting-edge technology in civil engineering community and gained increasing concerns all over the world (Lu *et al*. 2013, Ni *et al*. 2010, Lei *et al*. 2012a,b, Ni *et al*. 2012, Teng *et al*. 2015, Ye *et al*. 2012a,b, Ye *et al*. 2013a,b, Ye *et al.* 2014, Lei *et al*. 2015, Ye *et al*. 2015, Zhou *et al*. 2014, Zhou *et al*. 2015).

*Corresponding author, Associate Professor, E-mail: cexwye@zju.edu.cn
[a] MSc Student
[b] MSc Student

http://www.techno-press.org/?journal=sss&subpage=8 ISSN: 1738-1584 (Print), 1738-1991 (Online)

However, it is still a challenging task to precisely monitor/measure the cable force of the steel cables in long-span bridges.

Usually, the contact type methods are used to measure the tensile force of the steel cable. Measurement of the cable force by use of the load cell has the disadvantages that it must be mounted onto the anchorage of the cable and is inconvenient to replace and maintenance. The frequency-based system identification method can be employed to estimate the tensile force of the steel cable, but its measurement accuracy will be significantly affected by the boundary condition and bending rigidity of the steel cable (Ceballos and Prato 2008, Amabili *et al*. 2010, Li *et al*. 2014). Fiber Bragg grating (FBG) sensors are able to measure the structural force by transferring from the strain data when the optical fiber is closely stuck on the steel cable, while special attentions should be paid to the bonding condition between the FBG sensor and the steel cable (Kim *et al*. 2012, Lan *et al*. 2012, He *et al.* 2013). The force measurement methods based on the ultrasonic guided wave have been developed by many researchers, but the problems of electromagnetic interference and complex nonlinearity are existed (Lanza di Scalea *et al*. 2003, Chaki and Bourse 2009, Nucera and Scalea 2011). Another method for force monitoring of the steel cable is based on the reverse magnetostrictive effect through implementation of the electromagnetic stress sensor to identify the cable force by the relationship between the stress and the magnetic parameter (Bonchillonx *et al.* 1999, Joh *et al.* 2013, Yim *et al*. 2013), and the main drawbacks of this method are that the magnetic shielding and thermal effect will limit its stability and operational performance for online long-term monitoring.

In recent years, the machine vision technology has been rapidly developed with the aid of technological progress in digital image processing, which makes it become an alternative for performance monitoring of engineering structures (Choi *et al*. 2011, Jeon *et al.* 2014, Jurjo *et al*. 2015). Ye *et al.* (2015) proposed a method for multi-point structural displacement monitoring of bridges using a vision-based approach. Lee *et al*. (2012) developed a vision-based system for dynamic rotational angle measurement of large-scale civil engineering structures. Gales *et al*. (2012) employed the digital image correlation technique to determine the high-temperature deformation and stress variation of prestressing steel. Liu *et al.* (2014) developed a method for automated assessment of the cracks on concrete surfaces by use of adaptive digital image processing. Jahanshahi *et al*. (2011) evaluated the evolution of the structural defect using multi-image stitching and scene reconstruction.

With the help of high-precision multi-point structural displacement measurement, the force state of the steel structural component can be derived by the theory of elastic mechanics. This paper presents a non-contact vision-based cable force monitoring system based on the measured multi-point structural displacements. The effectiveness and accuracy of the proposed system has been validated through a series of laboratory experiments, including uniaxial tensile force tests of steel bars, steel wire ropes, and parallel strand cables on a universal testing machine (UTM) as well as a series of moving loading tests on an scale arch bridge model for measurement of the tensile force of the steel cable.

2. Vision-based method for non-contact cable force measurement

2.1 Multi-point pattern matching and structural displacement identification

For a vision-based structural displacement measurement system, the algorithm of multi-point pattern matching is able to effectively locate the targets in an image by matching the predefined patterns (Ye *et al*. 2015). Fig. 1 illustrates the flowchart of vision-based multi-point structural displacement measurement with the aid of multi-point pattern matching algorithm. First, an image with the identifiable target, T_0^i is captured by the digital camera, and the patterns containing the predesignated targets are extracted from the decent regions of the captured image. Meanwhile, the initial pixel coordinates of the centers of the patterns are recorded. Then, the scale ratio, r will be calculated, which represents the proportional relationship on the actual distance and the pixel coordinate difference between the target, T_0^i and the calibration reference point, R_0. Subsequently, the process of pattern matching is continuously performed between the predefined patterns and the succeeding images captured by the digital camera. Based on the correlation calculation (Ye *et al*. 2013b), a normalized correlation coefficient in correspondence with each pattern matching will be calculated. When the normalized correlation coefficient reaches the maximum value, the optimum matching position is deemed to be found, and the pixel coordinate of the center of the overlapped region between the pattern and the captured image is recognized. The pixel coordinate difference is obtained by subtracting the best matched pixel coordinate from the initial pixel coordinate. Finally, the structural displacement of the target is obtained through multiplying the calculated pixel coordinate difference by the scale ratio.

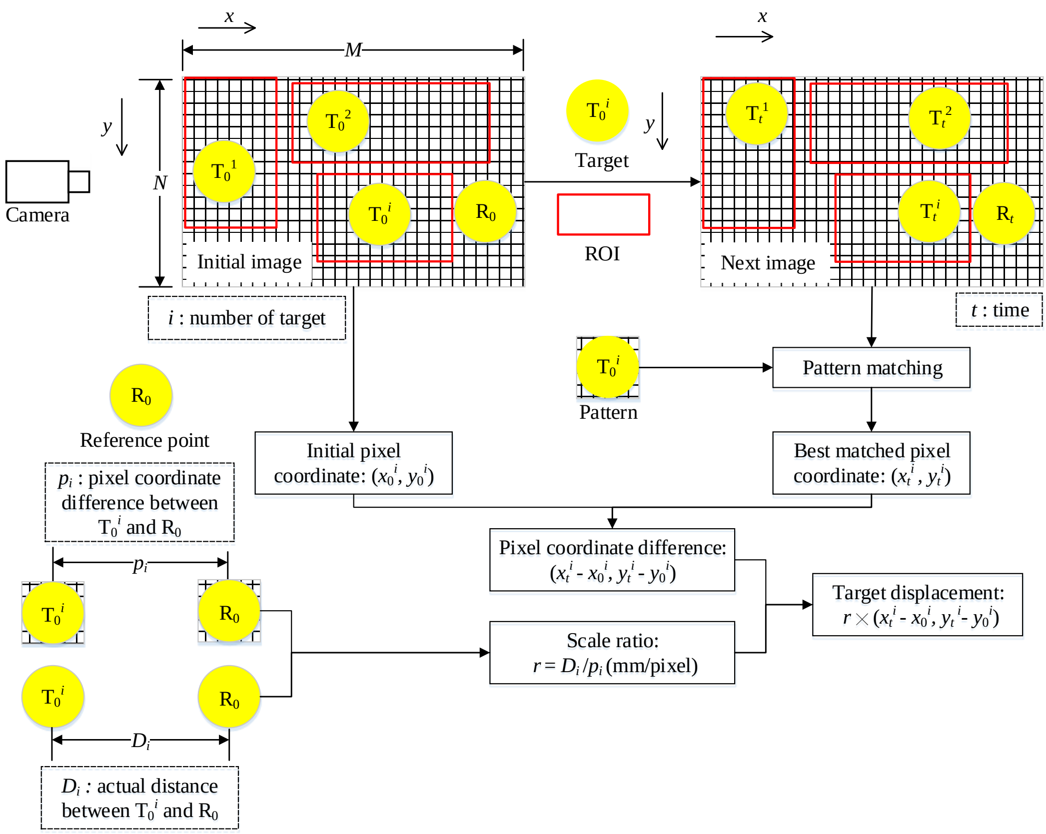

Fig. 1 Flowchart of vision-based multi-point structural displacement measurement

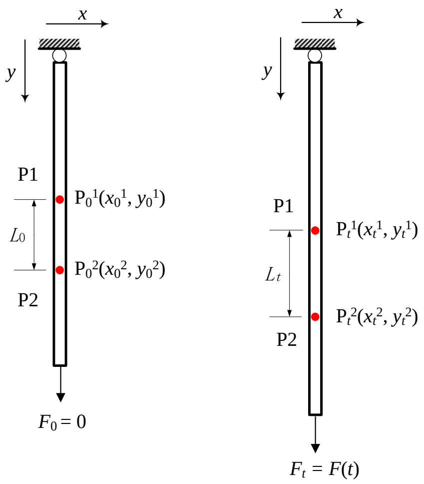

Fig. 2 Displacement-based cable force determination: (a) at time 0, (b) at time *t*

In the practical application and programming design, a region of interest (ROI) is used to improve the matching speed and operational efficiency. By presetting the ROI, the pattern matching and searching task are completed in this smaller region instead of the whole image area so that the unnecessary and irrelevant matching operations are eliminated. In the same time, the computer memory and CPU cycles are saved and consequently the pattern matching efficiency is increased. In addition, it will also improve the accuracy of target recognition and displacement measurement.

2.2. Displacement-based derivation of cable force

As illustrated in Fig. 2, with the purpose of monitoring the tensile force of the steel cable component, two measurement points (P1 and P2) are employed to estimate the vertical relative deformation which can be calculated by the displacements of the two points, and then the cable force, F_t will be derived. The relative deformation, ΔL and the strain, ε_t of the component between the two points (P1 and P2) from time 0 to t are calculated by

$$\Delta L = L_t - L_0 \tag{1}$$

$$\varepsilon_t = \frac{\Delta L}{L_0} = \frac{\left(y_t^2 - y_t^1\right) - \left(y_0^2 - y_0^1\right)}{y_0^2 - y_0^1} \tag{2}$$

where L_0 is the initial distance between P1 and P2; L_t is the distance between P1 and P2 at time t; y_0^1 and y_0^2 are the initial coordinates in the y direction of P1 and P2; and y_t^1 and y_t^2 are the coordinates in the y direction of P1 and P2 at time t.

According to Hooke's law, the sectional stress of the steel cable component, σ_t can be derived by

$$\sigma_t = E\varepsilon_t = E\frac{\left(y_t^2 - y_t^1\right) - \left(y_0^2 - y_0^1\right)}{y_0^2 - y_0^1} \tag{3}$$

where E is the Young's elastic modulus of the steel cable material.

Thus, the tensile force, F_t can be obtained by

$$F_t = \sigma_t A = EA\frac{\left(y_t^2 - y_t^1\right) - \left(y_0^2 - y_0^1\right)}{y_0^2 - y_0^1} \tag{4}$$

where A is the cross-sectional area of the steel cable component between the two points.

The determination of the tensile force of the steel cable component can be achieved by Eq. (4). The vertical structural displacements of P1 and P2 are measured by the vision-based system.

3. Experimental investigation of vision-based cable force measurement

As illustrated in Fig. 3, the vision-based multi-point structural displacement measurement system consists of a high-resolution industrial charge-coupled device (CCD) camera, a zoom lens, a computer, and a Gigabit Ethernet standard LAN wire. In this system, a Prosilica GE1050 camera with a Navidar 12X zoom extender lens serves as the image acquisition equipment. In the experimental study, the specimens of three types of structural components (steel bars, steel wire ropes, and parallel strand cables) are fabricated for tensile force measurement. The specific experimental processes and result analyses will be described in the following sections.

3.1 Tensile test of steel bar

As illustrated in Fig. 4(a), a steel bar specimen is fixed on the UTM for tensile force measurement. The specimen, which is made of hot-rolled plain bar HPB300, is a cylindrical steel bar with a diameter of 10 mm and a length of 500 mm. Two LED lamps are installed on the surface of the specimen as the vision measurement targets. In this tensile test, the loading rate of the UTM is set to be 250 N/s. The loading-unloading path is from 0 kN to 18 kN and then from 18 kN to 0 kN. The sampling frequency of the vision-based system and the UTM is 50 Hz.

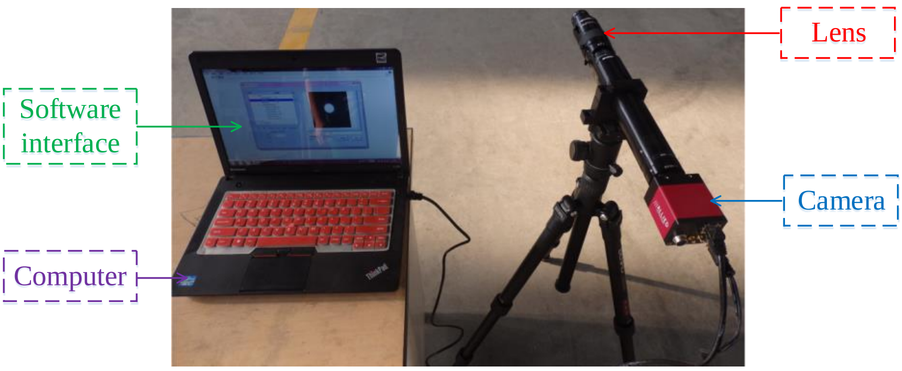

Fig. 3 Vision-based multi-point structural displacement measurement system

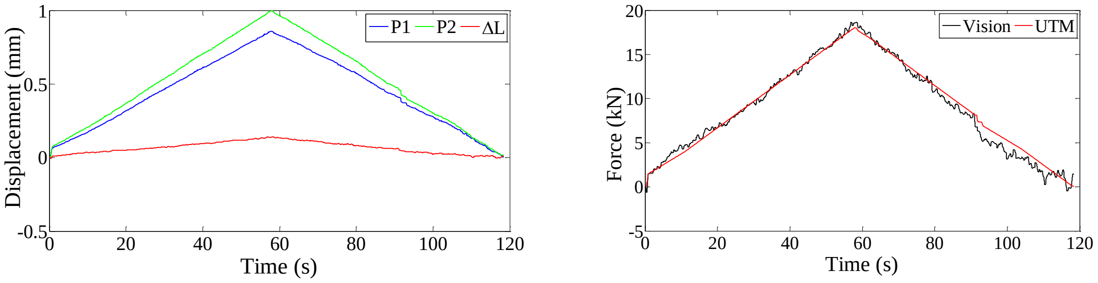

(a) (b)

Fig. 5 Measured displacements and forces of steel bar by vision-based system and UTM

Fig 5(a) shows the measured displacements of the two measurement points and the relative deformation of the structural component by the vision-based system. Based on Eq. (4), the tensile force of the steel bar can be calculated by use of the obtained relative deformation. It is seen from Fig. 5(b) that the derived tensile force of the steel bar is consistent with the force output from the UTM.

3.2 Tensile test of steel wire rope

As illustrated in Fig. 4(b), a specimen of steel wire rope is installed on the UTM for tensile force measurement. The specimen is categorized as the type of 6×7+IWS with a diameter of 5 mm and a length of 600 mm. Two LED lamps are deployed on the surface of the specimen as the vision measurement targets. In this tensile test, the loading rate of the UTM is set to be 50 N/s. The loading-unloading path is from 0 kN to 3.5 kN and then from 3.5 kN to 0 kN. The sampling frequency of the vision-based system and the UTM is 50 Hz. As illustrated in Fig. 6(a), the displacements of the two measurement points are measured by the vision-based system, and the relative deformation of the structural component can be obtained. Fig. 6(b) shows the calculated tensile force of the steel wire rope based on Eq. (4) and the force output from the UTM, and a good agreement can be observed between these two types of force measurement systems.

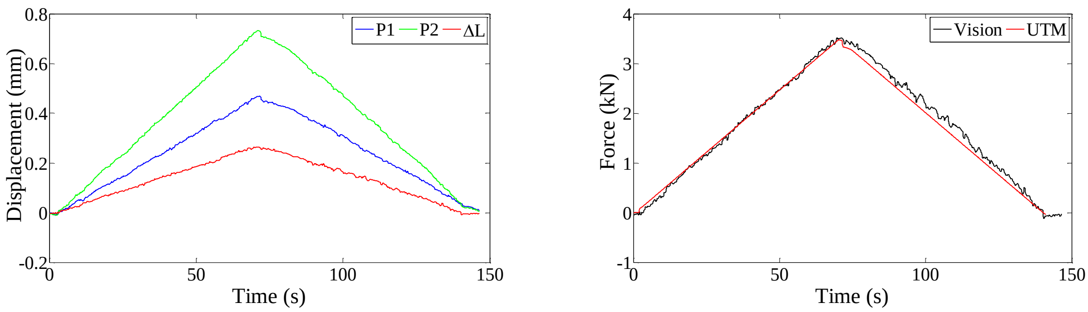

(a) (b)

Fig. 6 Measured displacements and forces of steel wire rope by vision-based system and UTM

3.3 Tensile test of parallel strand cable

As shown in Fig. 7, a parallel strand cable specimen is anchored on the UTM for tensile force measurement. This parallel strand cable comprises seven 7-wire epoxy-coated prestressed steel strands with a diameter of 15.2 mm. The individual wire is cold-drawn with a diameter of 5 mm and the tensile strength is 1,860 N/mm^2. The UTM is a computer-controlled electro-hydraulic servo multi-function testing machine, which is able to monitor the force and displacement in a real-time manner. An anchorage of the parallel strand cable is fully-customized to satisfy the requirement of the constraint condition during the process of loading-unloading cycle. Two LED lamps are deployed on the surface of one 7-wire strand as the vision measurement targets. In this tensile test, the loading rate of the UTM is set to be 5 kN/s. The loading-unloading path is composed of five cycles. In each cycle, the parallel strand cable is loaded by five loading levels from 0 kN to 800 kN, then unloaded from 800 kN to 0 kN. For each loading level (0 kN, 200 kN, 400 kN, 600 kN and 800 kN), the UTM is continuously operated for several minutes. During the interval of two adjacent loading levels, the parallel strand cable is loaded in a linear manner. The sampling frequency of the vision-based system and the UTM is 50 Hz. Fig. 8 illustrates the displacements of the two measurement points and the relative deformation of the structural component measured by the vision-based system. As shown in Fig. 9, the derived force results by the vision-based system are in consistence with those measured by the UTM.

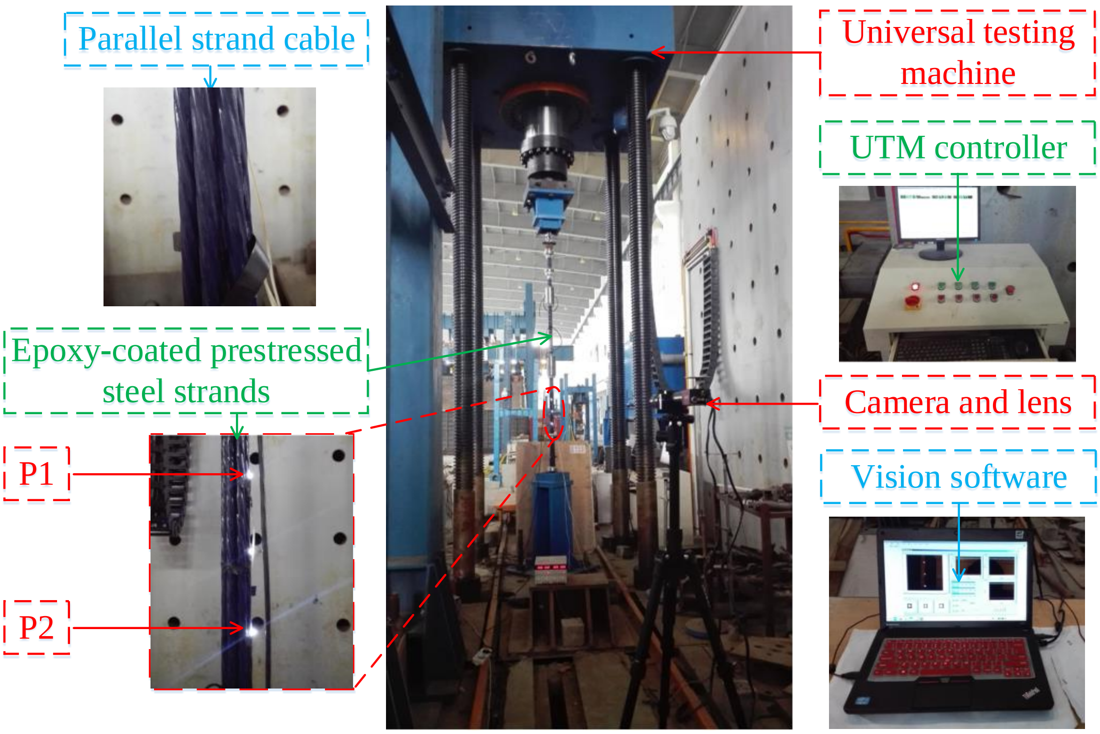

Fig. 7 Experimental setup of tensile test for parallel strand cable

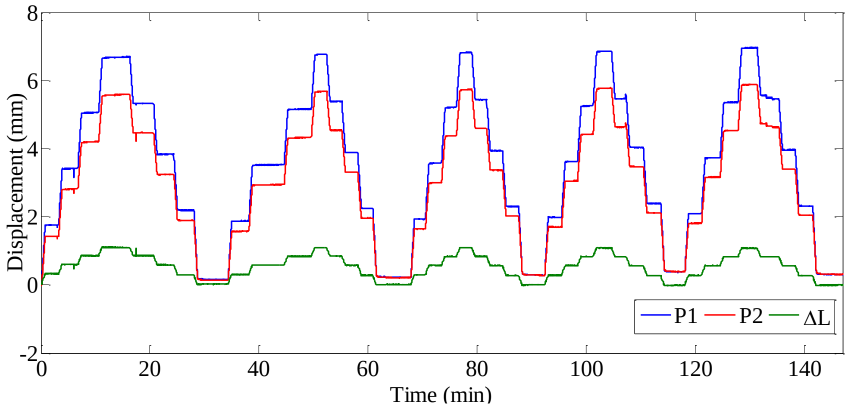

Fig. 8 Displacement time histories of parallel strand cable during 5 loading-unloading cycles obtained by vision-based system

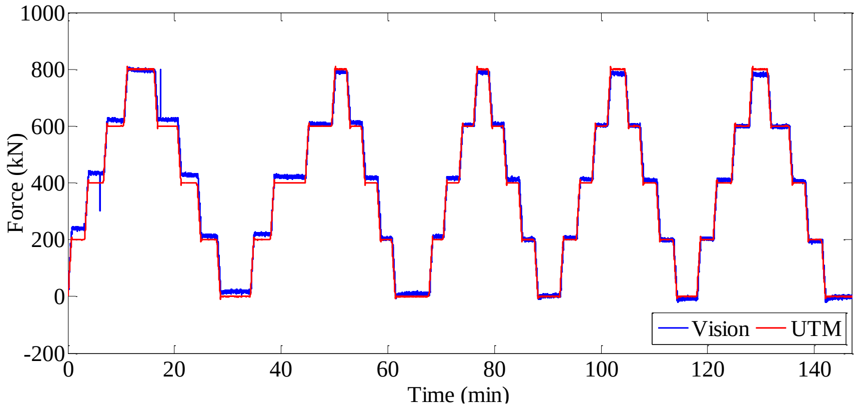

Fig. 9 Force time histories of parallel strand cable during 5 loading-unloading cycles obtained by vision-based system and UTM

3.4 Tensile test of steel cable on scale arch bridge model

As illustrated in Fig. 10, the scale arch bridge model is a half-through steel-tube arch bridge with a main span of 6 m and a deck width of 1.5 m which has been designed and fabricated as an integrated testbed for benchmark study of bridge health monitoring in Zhejiang University, China. For this scale arch bridge model, the longitudinal beams and crossbeams of the bridge deck system are assembled by rectangular steel tubes. Two main arch ribs are made by seamless circular steel tubes with a diameter of 70 mm and a wall thickness of 5 mm. The bridge deck is suspended by cables which are made of steel wire ropes with a diameter of 3 mm. 7 pairs of cables whose ends are anchored to the arch ribs and the side longitudinal beams are installed symmetrically with respect to the mid-span. Two rail tracks (south lane and north lane) are set on the deck of the scale arch bridge and a self-made test bogie acted as the loading device is used to simulate the moving loadings alike the highway traffic on the real bridge. Apart from the self-weight of the test bogie (5 kg), the counter weights with a known mass can be imposed on the test bogie to be as the additional weight during the moving loading experiments, and also the velocity of the test bogie can be adjusted.

In this experimental study, a steel cable at the mid-span of the scale arch bridge model adjacent to the north lane is chosen to conduct the tensile force measurement, which is the longest cable on the scale arch bridge model with a length of 900 mm and a diameter of 3 mm. As shown in Fig. 11, two LED lamps are deployed on the surface of the steel cable as the vision measurement targets. The upper end of the steel cable is fixed on the arch rib and the bottom end of the steel cable is clamped by a specially-fabricated screw. The screw is connected with a conventional contact-type *S*-type force sensor which is fixed on the deck of the scale arch bridge model to measure the tensile force of the steel cable. During the moving loading experiments, the bogie with a certain amount of counter weight will move through the deck of the scale arch bridge from the west side to the east side at different speeds. To verify the accuracy and effectiveness of the vision-based system, the tensile force of the steel cable also will be measured by the *S*-type force sensor with the same sampling rate of 50 Hz when the bogie moves through the deck on the north lane. Because the prestress force has been imposed on the steel cable during the assembling of the scale arch bridge model, the two measurement systems only will record the variation of the tensile force of the steel cable. Fig. 11 shows the experimental setup of the tensile test for the steel cable on the scale arch bridge model. Table 1 lists the loading conditions of the moving loading experiments with different loading masses and velocities of the bogie.

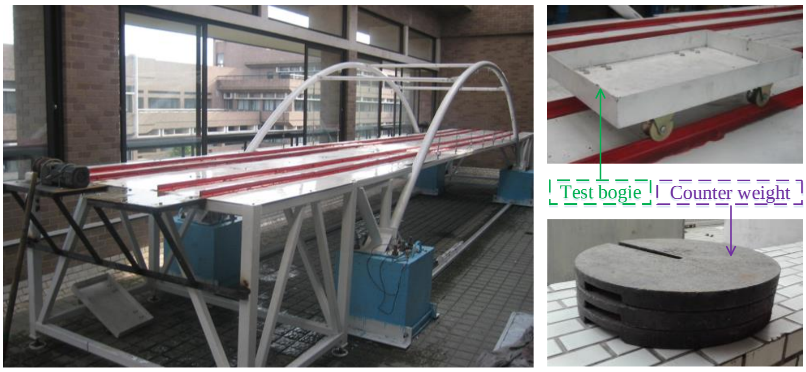

Fig. 10 Scale arch bridge model and moving loading system

Table 1 Loading conditions of moving loading experiments

Loading scenario	Loading mass (kg)	Velocity of bogie (m/s)
Case 1	85	0.40
Case 2	125	0.40
Case 3	165	0.40
Case 4	85	0.27
Case 5	125	0.27
Case 6	165	0.27

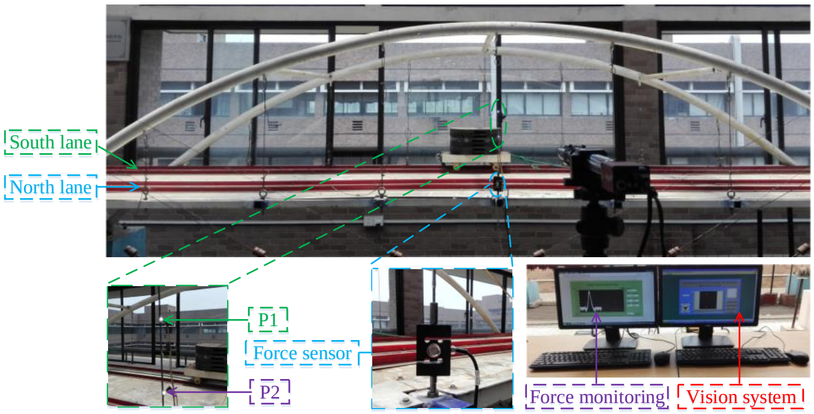

Fig. 11 Experimental setup of tensile test for steel cable on scale arch bridge model

Figs. 12-17 illustrate the measured displacement time histories of the two vision measurement points (P1 and P2) by the vision-based system for all cases as well as the derived force time histories calculated by the proposed method. It is seen from Figs. 12-17 that the tensile forces of the steel cable obtained by the vision-based system are basically matched with those measured by the force sensor. The amplitudes of the measured tensile force of the steel cable are changed with different loading masses and velocities of the bogie, and the shapes of the gained force curves are similar. The tensile forces of the steel cable reach the maximum value when the bogie approximately arrives at the mid-span of the scale arch bridge model.

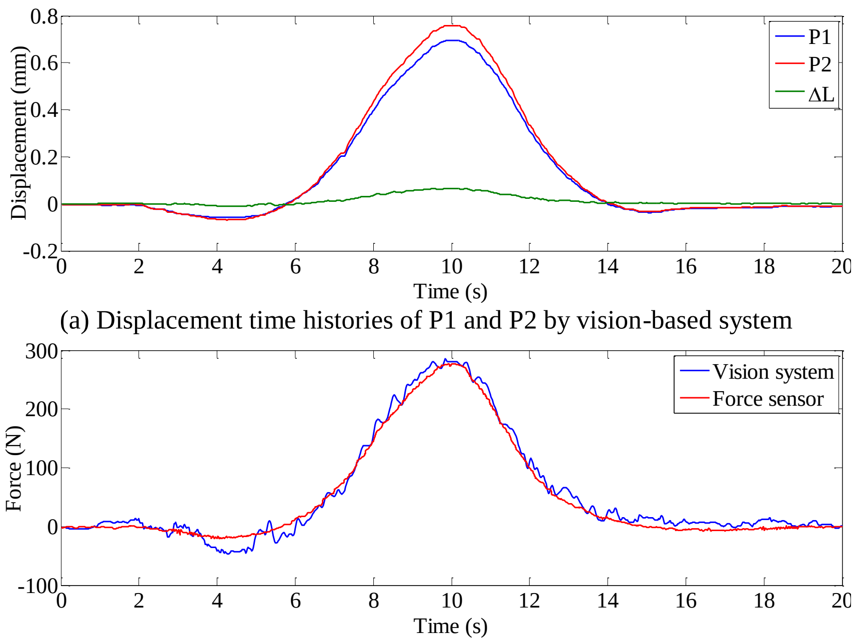

(b) Force time histories of steel cable obtained by vision-based system and force sensor

Fig. 12 Comparative analysis of measured results of Case 1

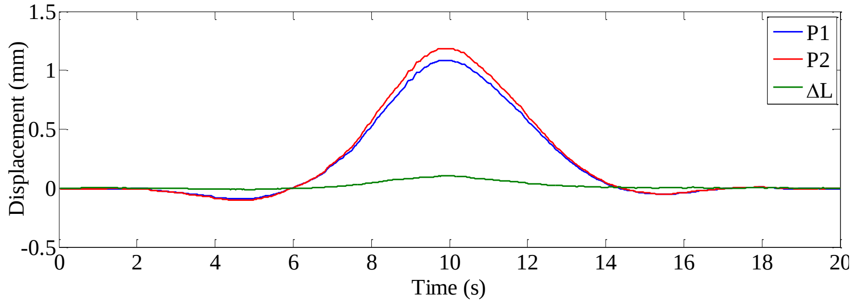

(a) Displacement time histories of P1 and P2 by vision-based system

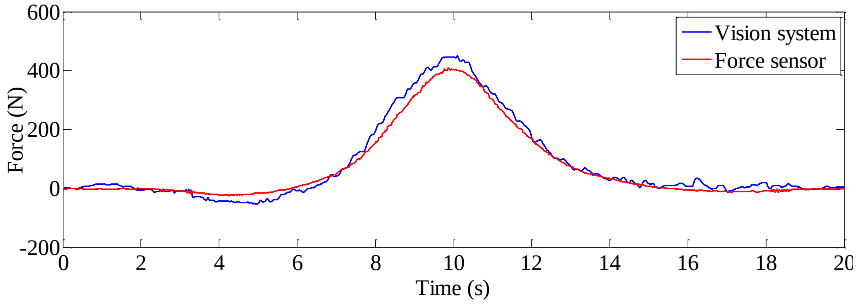

(b) Force time histories of steel cable obtained by vision-based system and force sensor

Fig. 13 Comparative analysis of measured results of Case 2

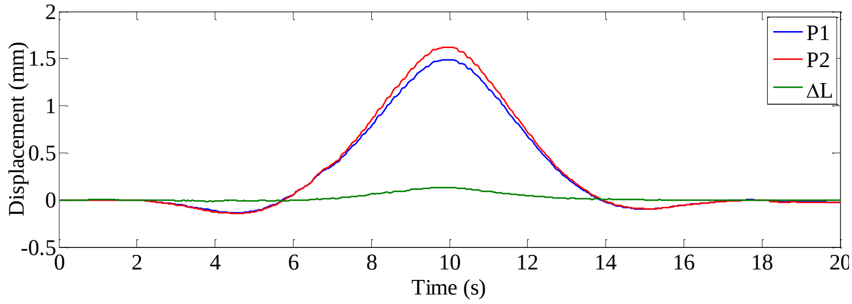

(a) Displacement time histories of P1 and P2 by vision-based system

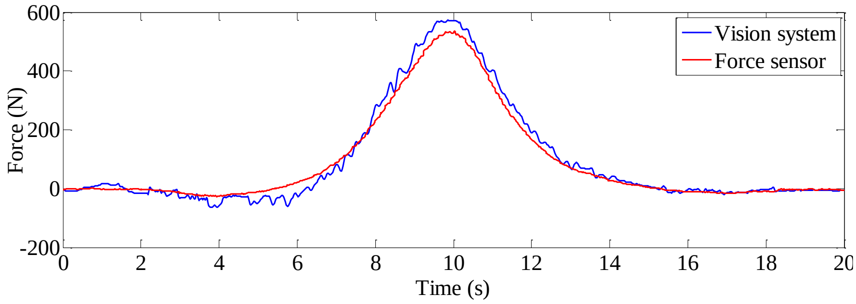

(b) Force time histories of steel cable obtained by vision-based system and force sensor

Fig. 14 Comparative analysis of measured results of Case 3

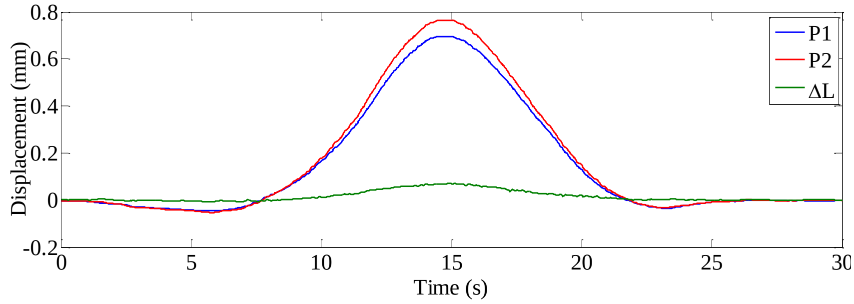

(a) Displacement time histories of P1 and P2 by vision-based system

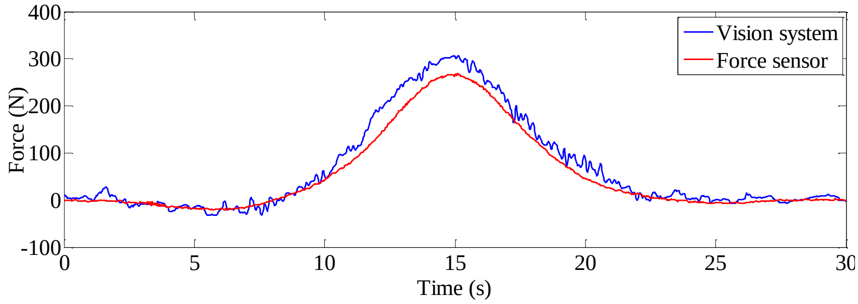

(b) Force time histories of steel cable obtained by vision-based system and force sensor

Fig. 15 Comparative analysis of measured results of Case 4

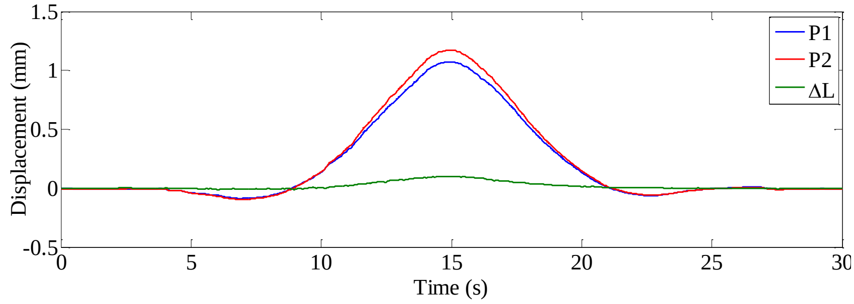

(a) Displacement time histories of P1 and P2 by vision-based system

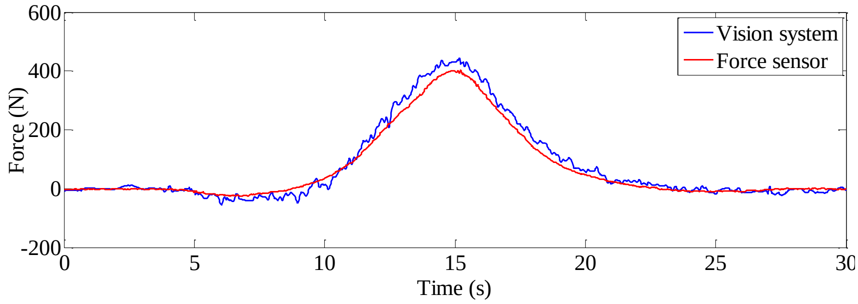

(b) Force time histories of steel cable obtained by vision-based system and force sensor

Fig. 16 Comparative analysis of measured results of Case 5

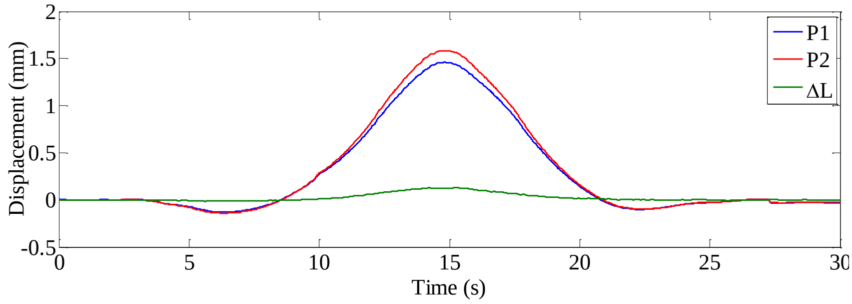

(a) Displacement time histories of P1 and P2 by vision-based system

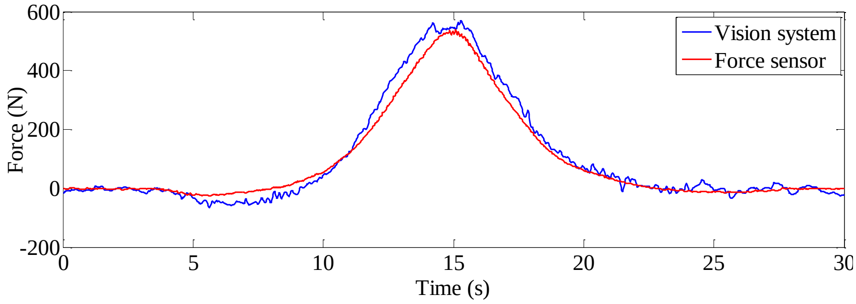

(b) Force time histories of steel cable obtained by vision-based system and force sensor

Fig. 17 Comparative analysis of measured results of Case 6

4. Conclusions

This study addressed the methodology and experimental verification of a vision-based system for force monitoring of steel cables in civil engineering structures. The uniaxial tensile tests of steel bars, steel wire ropes, and parallel strand cables on a UTM were carried out to validate the performance and accuracy of the developed vision-based system. Based on the laboratory experimental results, it is concluded that the vision-based system enables non-contact and high-precision force measurement of steel cables and may be a good alternative for cable force monitoring. In the near future, field experiments will be conducted to verify the accuracy and stability of the developed vision-based system in long-term cable force monitoring.

Acknowledgments

The work described in this paper was jointly supported by the National Science Foundation of China (Grant Nos. 51308493 and U1234204) and the Research Fund for the Doctoral Program of Higher Education of China (Grant No. 20130101120080).

References

Amabili, M., Carra, S., Collini, L., Garizera, R. and Panno, A. (2010), "Estimation of tensile force in tie-rods

using a frequency-based identification method", *J. Sound Vib.*, **329**, 2057-2037.
Bonchillonx, P., Lhermet, N. and Claeyssen, F. (1999), "Electromagnetic stress sensor for bridge cables and prestressed concrete structures", *J. Intel. Mat. Syst. Str.*, **10**, 397-401.
Ceballos, M.A. and Pratto, C.A. (2008), "Determination of the axial force on stay cable accounting for their bending stiffness and rotational end restraints by free vibration tests", *J. Sound Vib.*, **317**, 127-141.
Chaki, S. and Bourse, G. (2009), "Guided ultrasonic waves for non-destructive monitoring of the stress levels in prestressed steel strands", *Ultrasonics*, **49**, 162-171.
Choi, H.S., Cheung, J.H., Kim, S.H. and Ahn, J.H. (2011), "Structural dynamic displacement vision system using digital image processing", *NDT & E Int.*, **44**, 597-608.
Gales, J.A., Bisby, L.A. and Stratford, T. (2012), "New parameters to describe high-temperature deformation of prestressing steel determined using digital image correlation", *Struct. Eng. Int.*, **22**(4), 476-486.
He, J.P., Zhou, Z. and Ou, J.P. (2012), "Optic fiber sensor-based smart bridge cable with functionality of self-sensing", *Mech. Syst. Signal Pr.*, **35**, 84-94.
Jahanshahi, M.R., Masri, S.F. and Sukhatme, G.S. (2011), "Multi-image stitching and scene reconstruction for evaluating defect evolution in structures", *Struct. Health Monit.*, **10**(6), 643-657.
Jeon, H.M., Kim, Y.J., Lee, D.H. and Myung, H. (2014), "Vision-based remote 6-DOF structural displacement monitoring system using a unique maker", *Smart Struct. Syst.*, **13**(6), 927-942.
Joh, C., Lee, J.W. and Kwahk, I. (2013), "Feasibility study of stress measurement in prestressing tendons using villari effect and induced magnetic field", *Int. J. Distrib. Sens. N.*, **2013**, Article ID 249829, 1-8.
Jurjo, D.L.B.R., Magluta, C., Roitman, N. and Gonçalves, P.B. (2015), "Analysis of the structural behavior of a membrane using digital image processing", *Mech. Syst. Signal Pr.*, **54-55**, 394-404
Kim, B.H. and Park, T. (2007), "Estimation of cable tension force using the frequency-based system identification method", *J. Sound Vib.*, **304**, 660-676.
Kim, J.M., Kim, H.W., Park, Y.H., Yang, I.H. and Kim, Y.S. (2012), "FBG sensors encapsulated into 7-wire steel strand for tension monitoring of a prestressing tendon", *Adv. Struct. Eng.*, **15**(6), 907-917.
Lan, C.J., Zhou, Z. and Ou, J.P. (2012), "Full-scale prestress loss monitoring of damaged RC structures using distributed optical fiber sensing technology", *Sensors*, **12**, 5380-5394.
Lanza di Scalea, F., Rizzo, P. and Seible, F. (2003), "Stress measurement and defect detection in steel strands by guided stress waves", *J. Mater. Civ. Eng.*, **15**, 219-227.
Lee, J.J., Ho, H.N. and Lee, J.H. (2012), "A vision-based dynamic rotational angle measurement system for large civil structures", *Sensors*, **12**, 7326-7336.
Lei, Y., Chen, F. and Zhou, H. (2015), "An algorithm based on two-step Kalman filter for intelligent structural damage detection", *Struct. Control Health Monit.*, **22**(4), 694-706.
Lei, Y., Jiang, Y.Q. and Xu, Z.Q. (2012a), "Structural damage detection with limited input and output measurement signals", *Mech. Syst. Signal Pr.*, **28**, 229-243.
Lei, Y., Wang, H.F. and Shen, W.A. (2012b), "Update the finite element model of Canton Tower based on direct matrix updating with incomplete modal data", *Smart Struct. Syst.*, **10**(4-5), 471-483
Li, H., Zhang, F.J. and Jin, Y.Z. (2014), "Real-time identification of time-varying tension in stay cables by monitoring cable transversal acceleration", *Struct. Control Health Monit.*, **21**, 1100-1117.
Liu, Y.F., Cho, S.J., Spencer, Jr. B.F. and Fan, J.S. (2014), "Automated assessment of cracks on concrete surfaces using adaptive digital image processing", *Smart Struct. Syst.*, **14**(4), 719-741.
Lu, W., Teng, J. and Zhu, Y.H. (2013), "Diagnostic and recovering on spatially distributed acceleration using consensus data fusion", *Smart Struct. Syst.*, **12**(3-4), 271-290.
Ni, Y.Q., Ye, X.W. and Ko, J.M. (2010), "Monitoring-based fatigue reliability assessment of steel bridges: analytical model and application", *J. Struct. Eng. - ASCE*, **136**(12), 1563-1573.
Ni, Y.Q., Ye, X.W. and Ko, J.M. (2012), "Modeling of stress spectrum using long-term monitoring data and finite mixture distributions", *J. Eng. Mech. - ASCE*, **138**(2), 175-183.
Nucera, C. and Lanza di Scalea, F. (2011), "Monitoring load levels in multi-wire strands by nonlinear ultrasonic waves", *Struct. Health Monit.*, **10**(6), 617-629.
Teng, J., Lu, W., Wen, R.F. and Zhang, T. (2015), "Instrumentation on structural health monitoring systems

to real world structures", *Smart Struct. Syst.*, **15**(1), 151-167.
Ye, X.W., Ni, Y.Q. and Xia, Y.X. (2012b), "Distributed strain sensor networks for in-construction monitoring and safety evaluation of a high-rise building", *Int. J. Distrib. Sens. N.*, **2012**, Article ID 685054, 1-13.
Ye, X.W., Ni, Y.Q. and Yin, J.H. (2013a), "Safety monitoring of railway tunnel construction using FBG sensing technology", *Adv. Struct. Eng*., **16**(8), 1401-1409.
Ye, X.W., Ni, Y.Q., Wai, T.T., Wong, K.Y., Zhang, X.M. and Xu, F. (2013b), "A vision-based system for dynamic displacement measurement of long-span bridges: algorithm and verification", *Smart Struct. Syst.*, **12**(3-4), 363-379.
Ye, X.W., Ni, Y.Q., Wong, K.Y. and Ko, J.M. (2012a), "Statistical analysis of stress spectra for fatigue life assessment of steel bridges with structural health monitoring data", *Eng. Struct.*, **45**, 166-176.
Ye, X.W., Su, Y.H. and Han, J.P. (2014), "Structural health monitoring of civil infrastructure using optical fiber sensing technology: A comprehensive review", *Sci. World J.*, **2014**, Article ID 652329, 1-11.
Ye, X.W., Yi, T.H., Dong, C.Z., Liu, T. and Bai, H. (2015), "Multi-point displacement monitoring of bridges using a vision-based approach", *Wind Struct.*, **20**(2), 315-326.
Yim, J., Wang, M.L., Shin, S.W., Yun, C.B., Jung, H.J., Kim, J.T. and Eem, S.H. (2013), "Field application of elasto-magnetic stress sensors for monitoring of cable tension force in cable-stayed bridges", *Smart Struct. Syst.*, **12**(3-4), 465-482.
Zhou, G.D., Yi, T.H. and Li, H.N. (2014), "Wireless sensor placement for bridge health monitoring using a generalized genetic algorithm", *Int. J. Struct. Stab. Dy.*, **14**(5), 1-21.
Zhou, G.D., Yi, T.H., Zhang, H. and Li, H.N. (2015), "Energy-aware wireless sensor placement in structural health monitoring using hybrid discrete firefly algorithm", *Struct. Control Health Monit.*, **22**, 648-666.